MODELS AND TECHNOLOGIES OF EXPERIMENTAL STUDIES OF PROPERTIES OF INHOMOGENEOUS POWER STRUCTURAL ELEMENTS WITH OPTIMAL PARAMETERS

A.P. Dzyuba [1]   R.A. Iskanderov [2,3]   Y.M. Selivanov [1]

1. Oles Honchar Dnipro National University, Dnipro, Ukraine, dzb@ua.fm, selivanov-dnu@i.ua
2. Azerbaijan University of Architecture and Construction, Baku, Azerbaijan, r.iskanderov@gmail.com
3. Azerbaijan Technical University, Baku, Azerbaijan, ramiz.iskenderov@aztu.edu.az

Abstract- The results and technology of experimental studies using polarization-optical methods and holographic interferometry of the properties of load-bearing elements of thin-walled structures with optimal parameters are presented: circular frames, local increase in wall thickness, ribs that are used to reinforce cylindrical shells in places of concentrated force loading. The features of the stress-strain state, buckling and fracture are studied, as well as the results of a comparative analysis of the behavior of such power elements of optimal shape and constant cross-section of their equal weight are shown. It is shown that for power elements of optimal variable stiffness, higher strength and stiffness indicators are characteristic in comparison with the same elements of constant section, made from the same amount of material. New data have been obtained on the features of the processes of buckling of shells and the destruction of the optimal shape of the power frames that reinforce them, which consist in equalizing the distribution of stresses, reducing their maximum values, as well as the difference in the nature of destruction. On the example of a ribbed flat panel and a gearbox and clutch housing of a car, a methodology for a theoretical-experimental approach based on the application of holographic interferometry methods to the rational distribution of the material of real hull structures of a complex configuration is constructed. The research results are presented in the form of graphs and patterns of stress distribution, buckling, failure and comparative analysis data.

Keywords: Power Elements of Shells; Experimental Studies; Optimal Parameters; Photoelasticity; Holographic Interferometry.

1. INTRODUCTION

Experimental studies in deformable solid mechanics are one of important components of the successful solution of the problems of design, calculation and creation of the design of new technology. The main goals of such studies are to substantiate the reliability of the used mathematical models, theoretical and numerical calculations; conducting exploratory experimental studies aimed at studying individual mechanical aspects; building theoretical – experimental methodologies for the case when the possibilities of reliable structural modeling of the studied structural elements are complicated for various reasons and also carrying out full-scale, as a rule, destructive, as a result, rather expensive tests to verify the strength of the reliability of real structures as a whole.

There are a significant number of works devoted to the statements of methods, technologies and results of experimental studies: theoretical – experimental methods for studying thin-walled constructions of rocket space technology were applied in [1]; for aviation technology in [2]; for the protective shell of a power unit in [3]; for complicated structure hull structures in [4]; for the power structure of car in [5]; for spatial and cable-stayed constructions in [6]; for complex mechanical engineering systems in [7, 8]. Discussion of the results of experiments to determine the stability of cylindrical shells with holes are given in [9], destruction of shells with randomly located cuts-cracks in [10]. The use of the methods holographic interferometry is represented in [11–13], of polarizational-optical in [14].

At the same time, the results of experimental studies of power structural elements with optimal parameters, despite the undeniable urgency of optimal design of constructions [15-21] were not covered in well-known publications. When designing and studying the features of constructions with optimal parameters, theoretical methods are traditionally predominant, followed by an analysis of the results obtained numerically. And although at the same time, theoretical calculations and the results of solving the problem of optimal design indicate significant advantages of optimal structures with inhomogeneous parameters, their practical application is still problematic. The reasons for this state, among others, are both the complication of the technology of manufacturing products with irregular parameters and an increase in their cost as well as a certain distrust in the mechanical usefulness of such projects. The goal of this paper is a comparative analysis of the features of the stress-strain state (SSS) of power structural elements, and also to demonstrate the advantages of such designs by experimentation compared to test data of the original non-optimal construction.

2. INVESTIGATION OF WEIGHT-OPTIMIZED FRAMES OF CYLINDRICAL SHELLS

To strengthen shell and plate structures in the zone of their local transverse loading, ribs, linings, frames, or local thickenings of the wall are used. The development and application of weight optimization methods for such reinforcing power elements remain relevant. As is known [16, 22-24], the stress-strain state (SSS) of the frame strengthening the thin shell of rotation in the place of its loading by concentrated radial force, has an irregular character. Ensuring the strength of such a power frame by a general increase in its sizes leads to an unjustified power estimation of the weight of the structure. The use of power elements of the optimal variable along the length of the stiffening arc allows to improve significantly the characteristic parameters of SSS (to reduce stress or displacement in a structure or reduce its material consumption).

It should be noted that the solution of the problem of optimization of strength and stiffness features of such structures is characterized by a large number of restrictions imposed on the structure, variable parameters by the need to repeatedly solve the problem of conjugation of the shell and the frame of variable stiffness. As a rule, this requires some redistribution of material of the reinforcing elements. The papers [22, 23] with the results of experimental studies of the stress distribution in a frame with local stepped thickening and made of optic active material, and attached to the end of a long metal shell should be especially distinguished among publications devoted to experimental study of joint deformation of a power frame and cylindrical shell.

The subject of the research of this paper is a frame of rectangular variable in the circumferential direction of the cross-section, rigidly connected along the midline with the end face of the cantilevered cylindrical shell. The concentrated radial force was applied to the frame. The goal of the paper is to compare the SSS reinforcing the shell of optimal outline and constant section, equal weight frame with optimal one. Optimal, from the point of view of reducing the material consumption, the law of change in the height $h(\varphi)$ of the rectangular cross-section of the frame, variable in the circumferential direction of φ stiffness, is determined from the condition of minimum of the weight (volume) of the material, by the solution of optimal control problem using the Pontryagin maximum principle [25] in the following statement:

$$V_{opt} = \min_{h(\varphi)} \int_0^\pi 2\pi R\, b\, h(\varphi)\, d\varphi\,;\ \sigma(\varphi) \le [\sigma]\,;\ h(\varphi) \ge h_0 \quad (1)$$

allowing for the equations of joint deformation of a frame and shell [24]. Here R is a radius of the median line of the frame; b is the width of its cross-section; h_0 is the value of the lower design constraints;

$\sigma(\varphi) = M_{uu}(\varphi)/W_{uu}(\varphi) + N_{uu}(\varphi)/F_{uu}(\varphi)$ is the distribution of normal stresses on the contour of the frame; $[\sigma]$ is their allowed value; $M_{uu}(\varphi)$, $N_{uu}(\varphi)$ is a bending moment and longitudinal force in the frame under external radial loading with concentrated power P and forces of interaction with the shell; $W_{uu}(\varphi)$, $F_{uu}(\varphi)$ are the moment of resistance and cross-sectional area of the frame, respectively.

The sizes b, h_{const} of the cross-section of a constant stiffness frame were determined from the requirements of equality of the volumes of their material $V_{const} = V_{opt}$. Outlines of optimal configuration frames obtained by using the algorithm stated in [26] for the following parameters of the frame: $E = 2.9\,\text{GPa}$; $\sigma = 62\,\text{MPa}$; $R = 7.5 \times 10^{-2}\,\text{m}$; $b = 0.85 \times 10^{-2}\,\text{m}$; (a); $-h_0 = 0.3 \times 10^{-2}\,\text{m}$; (b); $-h_0 = 0.6 \times 10^{-2}\,\text{m}$; of the shell: $E_{sh} = 198\,\text{GPa}$; $\delta_{sh} = 3 \times 10^{-4}\,\text{m}$; $L = 0.15\,\text{m}$. for the cases of design constraints (a) and (b), are in Figure 1a and Figure 1b, where E, E_{sh} are elasticity modules of the frame and shell; δ_{sh}, L are the thickness of the wall and the length of the shell console, respectively.
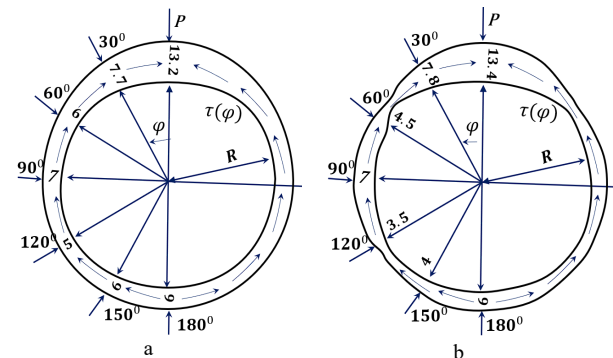

Figure 1. Configuration of the projects (a) and (b) of minimal weight frames

The advantages of projects of minimum weight frames with stiffness variable along the are length, was established in the experiments by comparing stresses and displacements in optimal variable frames along the length of the arc, and in constant cross section frames equal in weight, that reinforce thin elastic cantilevered cylindrical shell in the place of its loading with the concentrated radial force.

Comparison of the weight of the material of the optimal frame (a) and a frame of constant cross section equal to it in strength shows that the optimal one gives a gain in weight of 43.2%. Experimental studies were carried out using the polarization-optical method. The layout of the experimental setup is shown in Figure 2.
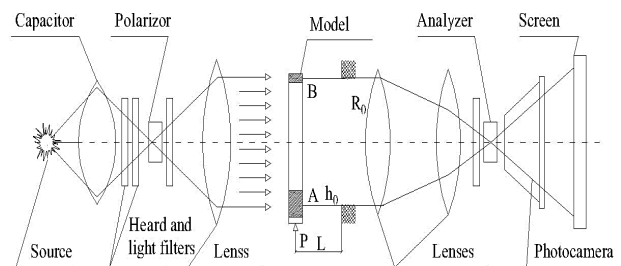

Figure 2. The scheme of polarization installation and test object

The application of the polarization-optical method is due not only to its relative simplicity, but also to possibility of comparative analysis of the stress strain state of the studied various configuration frames directly in the orders of the bands of the isochrome patterns. This avoids the errors caused by the calibration of the material, numerical integration and so on. Constant cross-section frames were made by turning on a lathe, while variable stiffness frames by means of locksmith tools from the blanks of plates of optically active material, obtained by the method of cold cured epoxy resin. The shells were made by a spot welding from the sheet steel X18H9n.

The frames were fixed on the shell along the neutral line. For the rigid connection of the end of a steel cylindrical shell with a frame in the latter (midline or reduced line), a circular groove of width of 0.8×10^{-3} m, was grinded on the half of its thickness, where the end of the shell freely entered. Before assembling, the groove was filled with epoxy glue of the same composition as the frame material. Polymerization of the bonding was conducted at a temperature of $50°C$ for four hours. There were no initial stresses with this connection method.

To ensure rigid built-in of the shell end opposite to the frame and possibility of illumination of both the outer and inner parts of the frame, a special device was made of high-quality interchangeable rigid boards and elements of their fastening to the test facility. The shell at a length 0.04m was fixed on the boards using epoxy glue. To one of the boards intended for studying the inner part of 0the frame, the shell was glued with the outer surface and this allowed to use frame to illuminate the space inside the shell. To the second board the shell was glued with the inner surface and this provided the possibility to illuminate the outer part of the frame Figure 3.
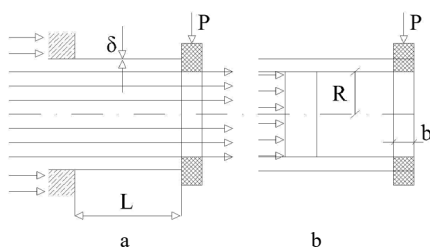

Figure 3. The scheme of illumination of the inner (a) and outer (b) part of the frame

The frames were illuminated with monochromatic light in the circular polarization mode. In order to exclude the blackout by shell of illuminated part of the frame the position of its axis was oriented in the direction of illumination. The loading of the model with radial power *P(for=0)*, directed from (or to) the center of the frame, was carried out in steps, increasing from 0 to failure of the construction, using edges of steel prism fixed on a rigid ring and oriented along the shell axis to transfer the force of the edges.

After the application of an external load, the patterns of the bands were observed on the installation screen, that were fixed on a contrasting photographic plate and served to determine the order of the bands and then the values of the normal stresses on the frame contour. The magnitude of the load at which the patterns of the bands were recorded should be taken the same for all tested frames taking into account the order of the bands and the bearing capacity of the structure. Normal stresses σ_k in illuminated parts of frames (taking into account that one of the principal stresses in the contour free from external loadings equals zero), were determined by the patterns of isochrome from the relation

$$\sigma_k = 2\, n_k \sigma_0 \qquad (2)$$

where, σ_k are stresses at an arbitrary point of the model contour; n_k is the order of the band; σ_0 is the model band price determined by the data of calculation test of material for pure bending.

Since all the frames were manufactured from the same batch of optical active material, then σ_0 was the same for all models, therefore, allowing for (2) the values of contour stresses can be compared directly in the band's orders. Stiffness characteristics of frames were established by measuring the radial displacements by means of a dial indicator at diametrically opposite points of the contour. A general view of the test device and the models under study are shown in Figure 4a.
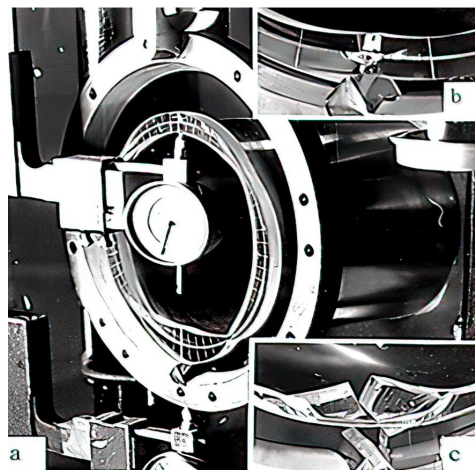

Figure 4. Tests (a) and destruction patters (b), (c) of the frame of a cylindrical shell under radial load

In the process of conducting experiments on band patterns, it was found that the highest contour stresses and highest orders of bands corresponding to them are concentrated in the area $|\varphi| \leq 45° \div 60°$. Therefore, comparative evolution of stresses in various type frames were conducted just in this area, since in the remaining sections the stresses were on average $2 \div 3$ times less.

The photos of the obtained isochrome patterns characterizing the stress of illuminated areas of frames in the zone of application of the load $P = 3.92$ H in the inner contour of the constant cross-section frame were represented in Figure 5, while in optimal outline frames for the case of structural constraints (a) and (b) in Figure 6 and Figure 7. These patterns show a significant thickening of lines in a constant section frame compared to the band patterns of optimal variable stiffness frames equal in

weight to them. Maximum band orders for the given loading are the bands $n = 11.2$ and $n = 5.2$, respectively.

All this indicates a gain in strength as a result of rational redistribution of the material of the frame. At the same time, the bands in the optimal frames were evenly distributed along the length of the arc in this interval. The value of normal stresses on the contours of frames were calculated by the isochrome patterns by means of 2.
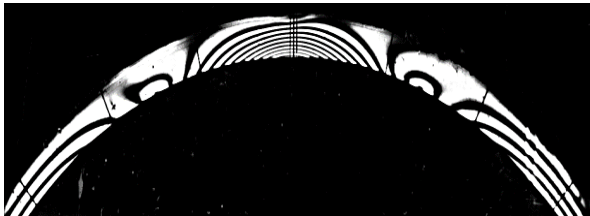

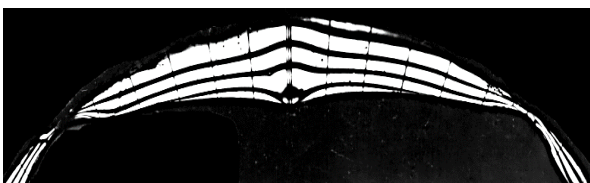Figure 5. Isochrome patterns in a constant cross-section frame

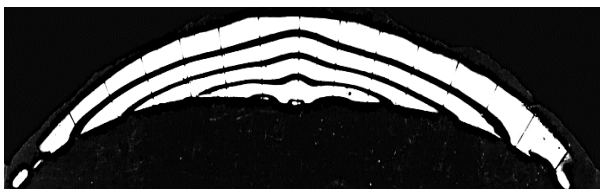Figure 6. Isochrome patters in a minimal weight frame (a)

Figure 7. Isochrome pattern in an optimal contour frame (b)

The experiment was repeated several times and photos of isochrome patterns were taken for various values of load. This time, the isochrome patterns were similar to ones given in Figures 5-7, and the frequency of isochrome lines changed proportionally to the load. The graphs of stress distribution on the inner contour of optimal frame (a) (line 1) and of constant cross section frame (line 2) for $0 \leq \varphi \leq \pi/2$ for $P = 3.92$ H, obtained due to the results of experimental studies and numerical calculations are given in Figure 8. This time it is seen that appropriate estimated values of σ_k (line 3, 4) for $-\pi/4 \leq \varphi \leq \pi/4$ agree well with the data obtained experimentally, the maximum values of σ_k in the zone of application of load in an optimal frame were event distributed and were $2.2 \div 2.4$ times less than in a constant stiffeners frame equal in weight.

We also note that the features of the optimal project can significantly change depending on the parameters of constraints. So, the isochrome pattern was given in Figure 7 while the graps of distribution of contour stresses in the zone of power ($P = 3.92$ H) in the optimal frame designed with regard to structural constraint (b): $h \geq h_0 = 6 \times 10^{-3}$ m (lines 5, 6, constructed similar to previous one, according to the results of the experiment and numerical calculation, respectively) Figure 8.
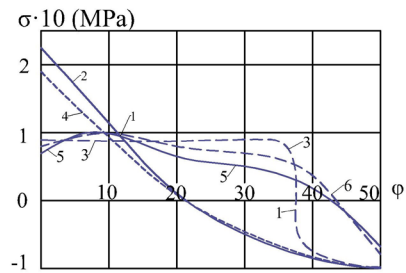

Figure 8. Stress distribution in the inner contour of frames (a) and (b)

In this case, the distractive load was almost the same (within the experimental error), but here such a uniform distribution of stresses is no longer observed as in Figure 6, there are unloaded sections. It should be taken into account that when solving the problems of designing minimal weight frames with regard to strength constraints and constructive requirements, at individual intervals, including zone of action of the force, there is an exit to the strength constraint boundary, that corresponds to the known properties of a discrete uniform tension $\sigma_k = [\sigma]$ [17], that here is just confirmed experimentally for optimal configuration frames.

On the part of the frame far from the applied load, the exist to the lower structural constraint is observed. This time stresses remain less than admissible and are distributed unevenly. This confirms that a minimum weight structure is not always equally stressed in the presence of constraints additional to strength conditions [17, 18].

3. INFLUENCE OF ECCENTRICITY OF FRAME LOCATION

The study is due to the greater practical applicability of schemes for conjugating a shell with a frame along the inner or outer surface of the shell. We considered the cases whose schemes are given in Figure 9, of symmetrical, external and internal location with respect to the shell of reinforcing optimal variable (1-3), rational variable (7-9) and constant (4-6) stiffness frame. All the frames under consideration had the same weight (volume) of the material.
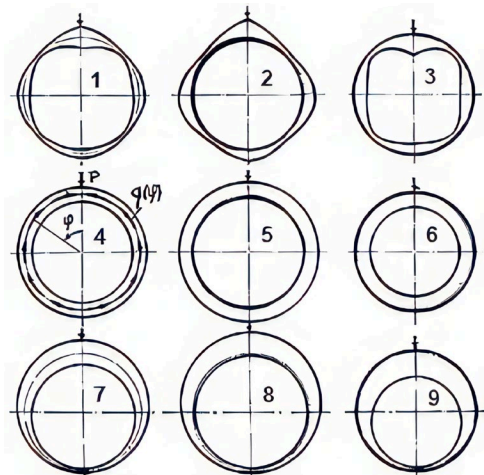

Figure 9. Configuration of equal weight frames with bilateral (1, 4, 7), external (2, 5, 8) and internal (3, 6, 9) with respect to shell material location

In the numerical solution of the direct problem of conjugation of the shell and frame [24] and further optimal distribution of the frame material as optimal control problems [25, 26] the deviation (eccentricity) of the form of the neutral line of a variable stiffness frame from the circular one was taken into account. Internal outline of constant stiffness frames with an external location (scheme 5, Figure 9) of the material and external outline of the frame (scheme 6, Figure 9) with its internal location, are the rings of radii $R-\Delta$ and $R+\Delta$, respectively ($\Delta = 1.25 \times 10^{-3}$ m).

And though with this method of fixing in the experiment, not all frame material was on one side (external or internal) of the shell (about 12% of the frame material still was located in the opposite side of the shell), this was a forced measure caused by considerations of the strength of gluing, since in the loading process, the structure was brought to destruction. Similar fastening of the frame on the shell was used for frames 1-3 and 7-9 as well.

In Figure 10 two characteristically isochrome patterns were given on the external contour of the optimal outline frame 2 (Figure 9) and of the constant stiffness frame equal to it in weight and adjoining to the point of application of radial force. The grasp of changes in contour stresses (in the band orders) on the external contour of frames in the action zone of power $P = 392$ H were given in Figure 11a. Stresses in minimal weight frames with symmetric (bilateral) and external fastening of the shell were given by curves 1, 2 respectively. Here, for comparison (curves 4, 5) the changes in stresses in appropriate constant section frames were given.
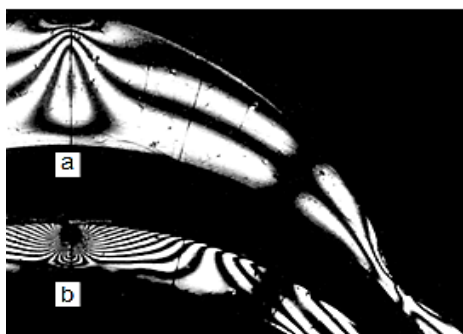

Figure 10. Isochrome patterns with external location of the material of frames: of optimal configuration (a), and of constant stiffness (b)

Distribution of contour stresses σ_k on the internal contour of frames was represented in Figure 11b (numbers of the curves correspond to the numbering schemes of frame in Figure 9). As in the previous experiments, contour stresses (in the most loaded area, in the immediate vicinity of the point of application of the radial force) at optimal configuration frames (lines 1, 2 in Figure 11a and lines 1, 3 in Figure 11b) distribution was more even and their maximum values were 2.2÷2.6 times less than in constant stiffness frames equal to them in weight (lines 4, 5 in Figure 11a and the lines 4, 6 in Figure 11b).
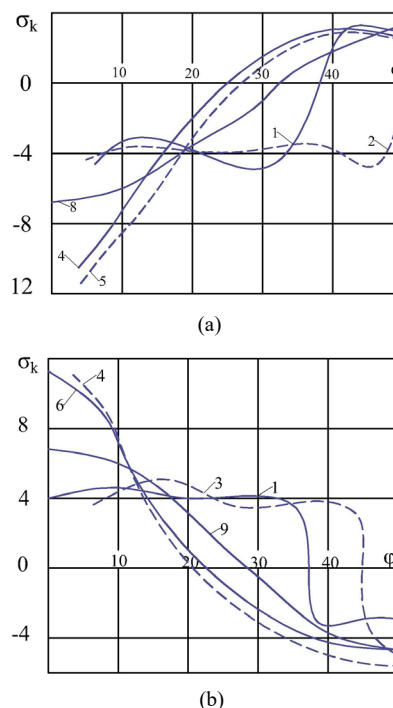

Figure 11. Stress distribution on external (a) and internal (b) contours of the frames

It is seen from the comparative analysis of the graphs of contour stresses distribution that (Figure 11) the transfer of the material of the reinforcing frame to the external or internal surface of the shell has little effect on the nature of the stress distribution, both for constant and optimal variable section frames.

At the same time, the ratio of the greatest stresses in constant section frames to the greatest stresses in appropriate optimal configuration frames increases (to 5–7%) with the transition from internal one to bilateral one and further to the external frame, that indicates an increase in the efficiency of using optimal form frames with the necessary reinforcement and corresponds to the results obtained in [27] for the case of a metal open rod.

Deformability of the shell was evaluated by indicators of dial gauges. Figure 12 shows the dependence of the approach value Δ of diametrically opposite points of vertical diameter of the frame on the change in the power P (number of lines correspond to the schemes of the frames in Figure 9).
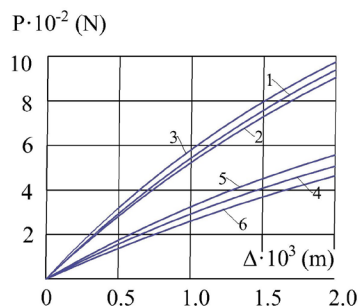

Figure 12. Coming together diametrically opposite points in the vertical section of the frame contour

It is seen from the obtained results that deformability of the shell edge when using an optimal configuration frame was 1.7÷1.9 times less than for a constant cross section frame. Despite the advantage of optimal variable stiffness frames, from the point of view of material consumption, strength and stiffness, their use is complicated by an increase in the cost of manufacturing technology.

Taking into account these aspects, further experimental studies of SSS were carried out for rational configuration frames whose contours were outlined by eccentric circles whose contours were drawn in such a way that the stiffness of the frame in the least loaded part (for $\varphi = \pi$) is determined from the limit structural constraint $h = h_0$, and in the remaining parts from the equality of the volumes of the used material.

The graphs of stress distribution on the external (internal) contour in eccentric structure frames were represented in Figure 11a, Figure 11b by the curves 8, 9, respectively. It follows from the obtained results that (compare the values of σ_k for $\varphi = 0$ of line 1, 2, 8 of Figure 4, and lines 1, 3, 9 of Figure 4b), according to the indicators of strength, stiffness and bearing capacity such projects of frames 1.5÷1.7 times exceed constant section frames and about 1.5 times yield to optimal configuration frames, while the manufacturing technology of such rational frames (Figure 9, schemes 7-9) is greatly simplified.

4. DESTRUCTION OF FRAMES AND SHELL BUCKLING

During the experiment, the structure under study was brought to destruction. It was established that the form of loss of bearing capacity of a cantilevered cylindrical shell stiffened with a frame has different character and depends on the ratio of stiffness of the shell and frame. The peculiarity of the loss of bearing capacity of the shell with a constant section frame was destruction of the frame as a result of appearance and development of a local crack under force (Figure 4b). The loss of bearing capacity of an optimal outline frame of the same weight happened almost simultaneously with its destruction at a considerable destruction in a relatively large area, including the point of application of force (Figure 4c), with perceptible sound effect.

Destructive force for two models of the constant cross-section frame was $P_p = 1.1 \times 10^3$ H and for optimal projects (a) and (b) $P_p = 2.4 \times 10^3$ H and 1.3×10^3 H, i.e. the bearing capacity of structures determined in the case under consideration by the destruction of the frame was significantly higher when using force elements of optimal configuration. Similar results were also obtained for optimal frames with ither parameters.

At the same time, it should be noted that at an optimal configuration frame, instead of one point dangerous for destruction (under the force) there arises a whole interval of such destruction causing points that in this sense decreases robust reliability of the optimal frame. This can be connected with, for example, appearance of some damage just in this zone. On the other hand, more than 2 times great value of destructive force allows in this case to introduce appropriate safety factor.

Then, the influence of the ratio of stiffnesses of the frame and the shell on critical load of the loss of bearing capacity of the tested model was studied. Instead of the sheet steel of mark X18H9n of thickness $\delta_{sh} = 0.3 \times 10^{-2}$ m for manufacturing the shell, the same steel of thickness $\delta_{sh} = 0.25 \times 10^{-2}$ m was used. The tests showed that in the case of a rational outline frame shape (scheme 8 of Figure 9), the loss of bearing capacity of the structure happened by the buckling of the shell (Figure 13).

Figure 13. Buckling of shell with transverse loading through frame

This time, critical force of buckling of such a shell was 1.6÷1.8 times greater than the loss of bearing capacity of the shell stiffened with a constant section frame as a result of appearance of a local crack and its destruction under the force. Thus, the destruction of a constant section frame stiffening the shell occurred before buckling of the shell, unlike the case of an optimal outline frame for which buckling of the shell occurred earlier. This corresponds to the results of the paper [27], where the stability constraint in the similar case also did not reveal its influence on the dimensions of the curvilinear rod.

Thus, the carried-out experiment illustrates the possibility of acquiring by the structure in the process of optimization a dangerous ability to violate constraints that are not typical for the original (non-optimal) structures of constraints (in this case buckling of the shell). Therefore, when setting an optimization problem, it is necessary to study preliminarily the features of behavior of the original non-optimal structure with regard to possibility of variation not only the sizes of the transverse section of the frame, but also the choice of rational parameters of the shell for revealing hidden constraints having a varied character (stiffness requirements, possibility of local buckling, appearance of stress concentrators, etc.).

The feature of the influence of stiffening elements with constant and optimal distribution of the material in the deflection field and buckling of a shell was further studied by the method of holographic interferometry. In this case, an optical scheme with maximum sensitivity to surface deflections was used [13]. Interferograms of the deflection field of the lateral surface of the shell stiffened with a frame of optimal outline (sample A) and of constant stiffness (sample B) in the process of its loading with the concentrated power P through the frame were given in Figure 14. The obtained interferograms give qualitative representation on the behavior of the shell in the process of its loading with the concentrated power P through the frame.

When increasing the power P from 0 to $540N$, the deformation character of the shell practically does not change in both stiffening cases. With further increase in power to 980 N, in the interferogram of the shell reinforced with an in optimal frame, we observe initiation of longitudinal dents (compare Figure 14 and Figure 13), that continue to grow for the values $P > 980N$ as well.

At the same time, the expected buckling of the shell did not occur, since the constant stiffness frame destructed before attaining the critical buckling force of the shell. This time, interference patterns of lateral surface of the shell reinforced with an optimal outline frame, remained practically unchanged before loads $P = (1.3 - 1.5) \times 10^3 \, \text{N}$ and only further for $P > 1.5 \times 10^3 \, \text{N}$ initiation of similar dents and buckling for $P = (1.7 - 1.8) \times 10^3 \, \text{N}$ was observed.
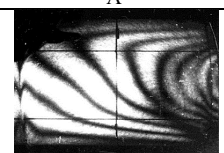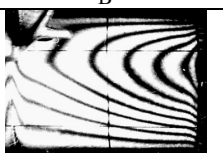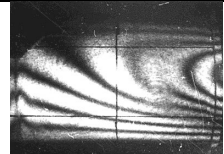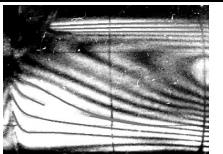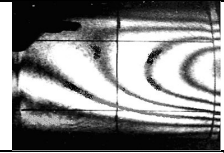
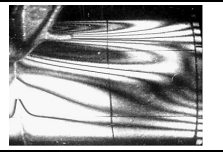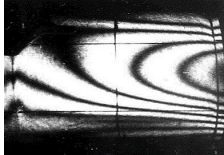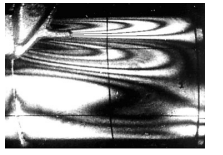| $P(\text{N})$	A	B
98		
490		
784		
980		

Figure 14. Interferograms of the lateral surface of the shells when loaded through the frame

The ultimate load for three pairs of identical samples A and B of the shell tested for destruction in the case of its reinforcement with an optimal outline frame was almost twice greater than for a constant section frame with the weight equal to optimal one.

5. OPTIMAL THICKENING OF THE SHELL WALL

The problem of weight optimization of an arbitrarily loaded shell of rotation with a stiffness variable in two directions is to find the thickness $h(s,\varphi)$ of the shell wall in the place of local radial loading from the condition of minimum volume of the material

$$V = \min \int_0^{2\pi} \int_{s_0}^{s_N} r(s) h(s,\varphi) \, ds \, d\varphi \qquad (3)$$

Subject to the state equations of the shell with boundary conditions for fixing the ends [28, 30] and in the presence of constraints of strength, stiffness and structural requirements, respectively:

$$\max \sigma_{eq}(s,\varphi,z) \leq [\sigma]$$
$$|\sigma_-| \leq \sigma_{kr}, \ \bar{u}(s,\varphi) \leq \bar{u}_{\max}, \ h_1 \leq h(s,\varphi) \leq h_2 \qquad (4)$$

Here, for calculating equivalent stress the following dependence is accepted:

$$\sigma_{eq} = \sqrt{\left(\sigma_1^2 + \sigma_2^2 - \sigma_1 \sigma_2 + 3\tau_{12}^2 + 3\tau_{1z}^2 + 3\tau_{2z}^2\right)/2},$$

where, $\sigma_1, \sigma_2, \tau_{12}, \tau_{1z}, \tau_{2z}$ are normal and tangential stresses in the sections of the shell, respectively; σ_{kr} are critical stresses of buckling determined according to [29]; $\bar{u}(s,\varphi)$ is a vector of components of SSS displacements; h_1, h_2 are the values of the lower and upper structural constraints and h_0 is the thickness of the wall of the constant stiffness shell.

In accordance with difference- differential approaches [28, 30] the Equation (3) by replacing integration over φ with summation is given in the form

$$V = \int_0^{2\pi} \int_{s_0}^{s_n} r(s) h(s,\varphi) \, ds \, d\varphi \approx \frac{2\pi}{M} \sum_{m=1}^{M} \int_{s_0}^{s_n} r(s) h(s,\varphi_m) \, ds =$$

$$= \frac{2\pi}{M} \int_{s_0}^{s_n} r(s) \sum_{m=1}^{M} h(s,\varphi_m) \, ds$$

where, $r(s)$ is the radius of the parallel circle of the shell; M is the number of nodes (discretization bands) in the circumferential direction. Thus, the optimal design problem is reduced to finding minimum of the functional

$$V^* = \int_{s_0}^{s_n} r(s) \sum_{m=1}^{M} h(s,\varphi_m) \, ds \qquad (5)$$

Representation of Equation (3) in the form of (5) for the object described by the system of $8 * M$ ordinary differential equations of state of a variable stiffness shell in the form [30] involving Equation (4) allows to apply to the initial two-dimensional problem the Pontryagin maximum principle in its one-dimensional form [25, 26].

Figure 15 shows optimal variable in two directions the distribution of stiffness, the reinforcement of the wall thickness of a hinged steel cylindrical shell $(X18H9n)$ (Figure 15a) in the longitudinal (Figure 15b) and in the transverse (Figure 15c) directions. The results were obtained for the following parameters: of radius $R = 0.057 \, \text{M}$, shell length $L = 2R$ and shell thickness $h_0 = 3 \times 10^{-3} \, \text{M}$ in the place of local radial loading with the power $P = 1.5$ N. Lines 1, 2, 3 correspond to the values of $[\sigma]$ in the constraints (4), equal to 100, 150, 200 MPa.

Compared to the case of a rectangular lining of constant thickness $h^* = h_0$ (Figure 15a) the stresses turned out to be almost twice as small with the same amount of the material max σ_{eq}. The shells for experimental studies were manufactured by spot electric welding from the sheet steel X18H9n of thickness $h_0 = 2.8 \times 10^{-4} \, \text{m}$, had a radius $R = 0.057 \, \text{M}$ and a working length $L = 2R$.
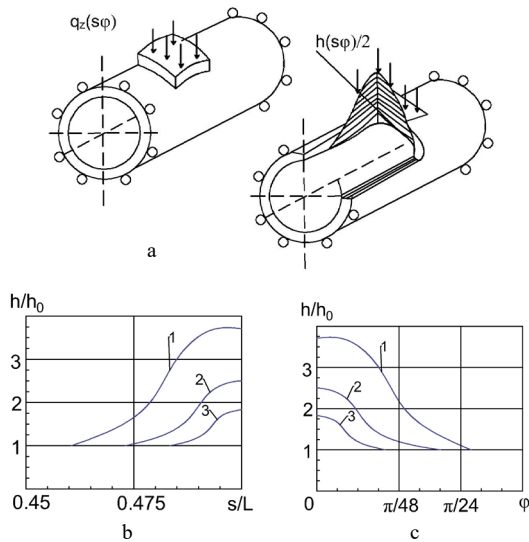
Figure 15. Designing optimal thickening of the shell wall

Behavior of three models of the shells built in at the ends, was studied by the method of holographic interferometry. The first model was a flat cylindrical shell without reinforcement. The second model was a cylindrical shell reinforced by a lining of thickness h_0, the third one had an optimal configuration local thickening in the area of application of concentrated radial power. The linings were also manufactured from the steel X18H9n.

Local thickening of the optimal configuration was performed in the form of three layers of thickness h_0 (Figure 16 it was distinguished by rectangles) connected between themselves by special hard glue. The lining was attached to the shell with the same glue. The loading was carried out using dimensional loads, of the block and flexible traction one end of which was fixed on the shell at the point of application of power preliminarily passing through a small hole in the diametrically opposite zone of the shell.
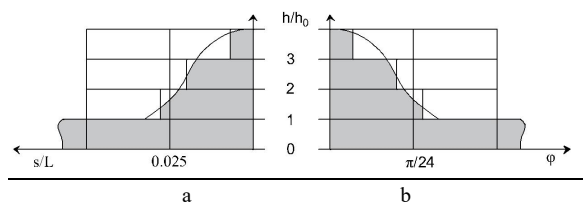

Figure 16. Modeling of optimal distribution of the thickness of the shell wall in the force zone in the longitudinal (a) and circumferential (b) sections

The registration of interferograms was carried out using the optical scheme of central illumination and observation. Holographic interferograms of the tested models were given in Figure 17. The deflection w recorded on the interferogram was determined by the formula.

$$w = \frac{2}{\lambda N (\cos\theta \cdot \cos\psi)} \tag{6}$$

where, λ is the wavelength of the radiation used; N is the order of the interference fringe at a given point on the shell surface; θ is half of the angle between the directions of illumination and observation of the surface at a given point; ψ is the angle between the deflection direction and the bisector of angle 2θ at this point.
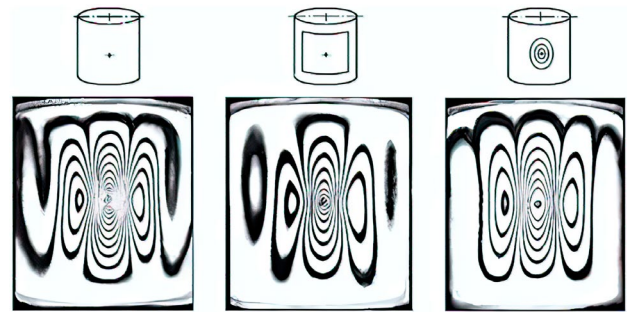

Figure 17. Holographic interferograms of the tested models when loaded with radial power $P = 1.5$ N

The values of deflections along the longitudinal and transverse sections passing through the point of application of the force, determined from these interferograms, are shown in Figure 18.
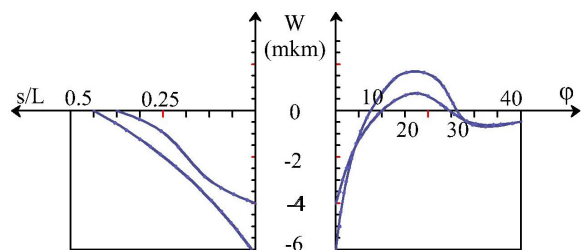

Figure 18. Distribution of deflection of the shell without reinforcement (solid curves) with an optimal lining (dashed)

Analysis of interferograms (Figure 17) shows the following. A square overlay of thickness h_0 and width 0.5 L had no noticeable effect on the character of this field. The absolute values of the deflections, as expected, decreased by half. The optimal lining, for the manufacture of which many times less material was spent, had almost the same effect on the maximum deflections (Figures 17 and 18). Evaluation calculations also showed that all parameters of the SSS structure as a whole improved.

Thus, application of holographic interferometry allows to assess the advantage of obtained optimal projects from the point of view of specific strength and stiffness, and also to demonstrate efficiency and expediency of their wide use in design practice.

6. PARAMETER OPTIMIZATION TECHNIQUE BASED ON EXPERIMENTAL DATA

This section demonstrates that, in a number of cases, a rational distribution of the material of inhomogeneous thin-walled structures can also be obtained experimentally, in particular, using the method of two-exposure holographic interferometry, without resorting to relatively complex theoretical methods and algorithms. Further, the application of the corresponding technique is shown on the example of a ribbed plate under bending by a transverse concentrated force.

The essence of the technique is as follows. Using holographic interferometry, the main stresses in the structure are determined (Section 5), and its equivalent stresses are estimated. In proportion to these stresses, material is removed or built up, respectively, in underloaded and overloaded areas. Further, in the resulting model, the equivalent stresses are again determined. According to the results of their analysis, the process of material redistribution continues until the difference between the determined stresses at all control points of the structure becomes less than the specified value.
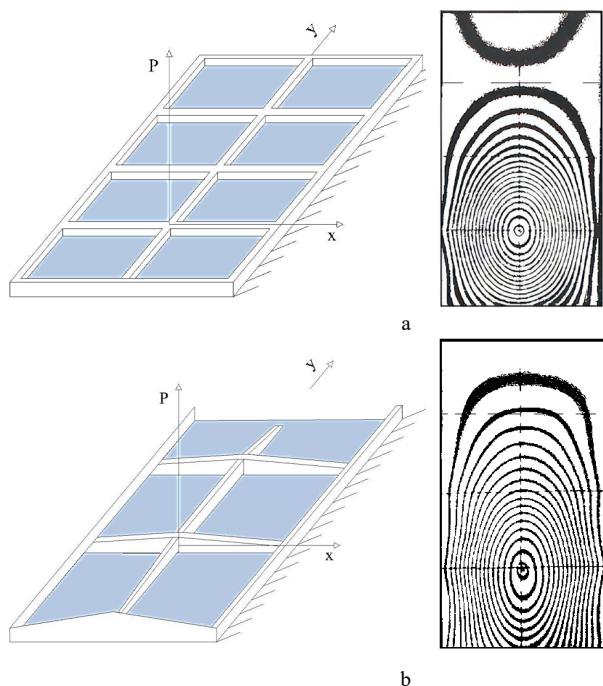

Figure 19. The scheme of ribbing and interferogram of the plate (from the smooth side) for $P = 3.2$ H in the initial state (a) and after the third change in the sections of ribs (b)

Approbation of the technique was carried out by on a model rectangular plate, made of Plexiglas (plate length 0.168 m, width 0.090 m, thickness 0.003 m), stiffened from one side by a central longitudinal and five equidistant transverse rectangular section stiffens ribs of height 0.010 m and of width 0.004 m (Figure 19a). The plate was rigidly clamped along the long sides, and loose along the short sides. Through one of the fin nodes, it was mechanically loaded by the concentrated force P.

To receive the interferograms, an optical scheme of central weakly spherical illumination and remote observation was used. The build-up and removal of the plate material was carried out only by increasing or decreasing the height of their section linearly along the length of the ribs.

On Figure 19 shows the interferograms of the plate with the initial distribution of the material and after the third change in the sections of the ribs. The interpretation of the interferograms was carried out according to Equation (6). As a result of interpretation of the interferograms, the distributions of the deflections of the plate models along the coordinate axes were constructed (Figure 20), the effective equivalent stresses were estimated.
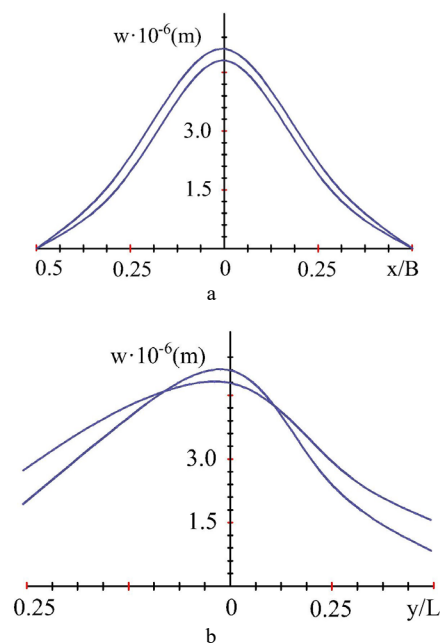

Figure 20. Distribution of plate deflections along the axis x (a) and y (b): solid lines correspond to the initial state; dashed lines show the state after the third change in the sections of the ribs; points are interferogram interpretation data

The obtained results testify that the suggested methodology with rather high effectiveness can be used for increasing strength and stiffness properties of inhomogeneous thin-walled structures experimentally.

The use of holographic interferometry for determining rational parameters of the structure then was demonstrated for the case of shell and plate structures more complicated in material distribution and technology of manufacturing, as gearbox housing and car clutch. Using a special device for loading and holographic device the infergograms of the crankcase surface in all gears were obtained. One of them is given in Figure 21. Distribution, of deflection increments in the most and least deformed areas in the directions of local principal curvatures were constructed according to interferograms.

Based on these data, similarly to previous one, specific recommendations for a rational change in the thickness of the crankcase wall allowing to reduce its weight were developed. It should be noted that when solving the problems on improving strength and stiffness qualities of such hull constructions as a crankcase using the experimental approach, their manufacturing technology carried out mainly by casting using a fairly expensive press form whose change in configuration is a significant obstacle to the implementation of the approach, should be taken into account.

Such an approach contains the obvious advantage of being able to significantly reduce the cost of reworking of appropriate press forms. The use of visual highly informative experimental data on displacement fields makes it possible to correct the finite element model of the structure at each optimization step and consequently, to increase the reliability of the results of determining SSS and rational parameters of the structure.
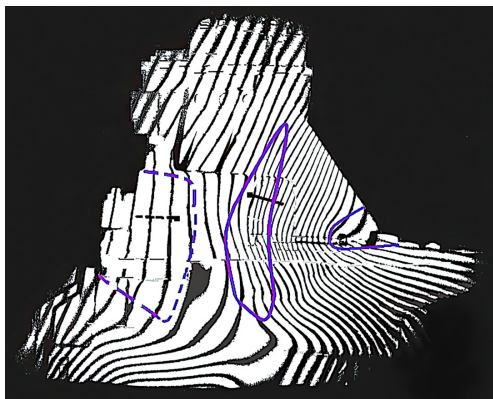
Figure 21. Holographic interferogram of the crankcase surface in «Reverse gear»

7. CONCLUSION

New data on the properties of a structures with force elements optimal in weight, have been obtained. This is a reduction in the maximum values and the equalization of the stress distribution, an increase in the bearing capacity and stiffness, differences in the nature of the loss of bearing destructive capacity (local crack, simultaneous destruction of a significant section of the frame, shell buckling, accounting for the effect of eccentricity). The reliability of the design methodology based on the methods of theory of optimal processes has been confirmed. The advantage of the obtained optimal projects has been evaluated. It has been demonstrated that for variable stiffness projects optimal in weight, higher strength and stiffness indicators compared to constant section structures made of the same amount of material are characteristic.

The methodology and results of experimental (using the methods of photoelasticity and holographic interferometry) studies, the properties of frames, linings, ribs and distribution of the thickness of the wall with constant and optimal parameters for stiffening shell and plates, have been given. The represented results of experiments can be useful for substantiating the reliability and assessing the accuracy of calculation methods and optimization algorithms, as well as directly for ensuring rational parameters of the shell and plate units of machines and constructions.

REFERENCES

[1] M.V. Marchuk., V.M. Sirenko, B.D. Drobenko, "Methodology for Determining Destructive Loads on Large-Sized Thin-Walled Structures, Taking into Account the Results of Non-Destructive Tests", Appl. Problems of Mechanics and Mathematics, Vol.18, pp.133-138, 2020.

[2] T.M. Laft, O.W. Hylon, N.M. Htel, I.V. Volkov, "Calculation Experimental Method for Analyzing the Stress Strain State (SSS) of Aircraft Structures", Trudy MPhTI., Vol. 10, No. 4. pp. 131-136, 2018.

[3] A. Bambura, I. Sazonova A. Karpenko, et al., "Experimental Researches of a Fragment of a Prestressed Protective Shell of a Power Unit of a Nuclear Power Plant", Nuclear and Radiation Safety, Issue 1, Vol. 89, No. 3, pp. 49-58, 2021.

[4] A.P. Dzyuba, Yu.M. Selivanov, "Research of Strength Characteristics and Optimization of Parameters of Case Structures Using Holographic Interferometry", J. Phys.: Conf. Ser. (JPCS), Vol. 1741, p. 012046, 2021.

[5] B.A. Kayumov, R.A. Vohobov, "Making Changes to the Design of Cars Based on Test Results", Bul. Sciences and Practices, Vol. 5, No. 11, pp. 249-254, 2019.

[6] L.I. Storozhenko, G.M. Hasii, "Methodology of Experimental Research of a Large-Sized Sample of a Spatial Structural and Cable-Stayed Steel-Reinforced Concrete Structure", Academic Journal Industrial Machine Building Civil Engineering, Issue 2, Vol. 49, pp. 270-276, 2017.

[7] N.A. Tkachuk, A.V. Khlan, A.I. Sheiko, et al., "Development of a Mathematical Apparatus for Solving Problems of Computational and Experimental Research of Elements of Mechanical Systems", Bulletin of NTU "KHPI" Series: Mechanical Engineering and CAD, Vol. 12, No. 1234, pp. 110-131, 2017.

[8] Yu.V. Veretelnik, A.V. Tkachuk, O.V. Kokhanov-skaya, et al., "Computer Modeling of Processes and States of Complex Systems: Substantiation of Model Parameters by Calculation and Experiment", Bulletin of NTU "KHPI" Series: Mechanical Engineering and CAD. Vol. 12, No. 1234, pp. 14-25, 2017.

[9] A.P. Dziuba, E.F. Prokopalo, P.A. Dzyuba, "Bearing Capacity of Cylindrical Shells with Holes: Monograph", Lira, p. 224, Dnipro, Ukraine, 2014.

[10] A.P. Dzyuba, P.A. Dzyuba, R.A. Iskanderov, "Numerical and Experimental Simulation the Destruction of the Stretched Cylindrical Shell Damaged by Random Cuts-Cracks", International Journal on Technical Physical Problems of Engineering (IJTPE), Issue 53, Vol. 14, No. 4, pp. 175-181, December 2022.

[11] T. Kreis, "Handbook of Holographic Interferometry: Optical and Digital Methods", Wiley-VCH Verlag Gmbh and Co., p. 542, 2005.

[12] I.V. Volkov "Using the Method of Speckle Holography in Experimental Mechanics", Izmeritelnaya Tekhnika., No. 2, pp. 42-46, 2017.

[13] V.S. Gudramovich, A.P., Dzyuba, Yu.M. Selivanov, "Methods of Holographic Interferometry in the Mechanics of Inhomogeneous Thin-Walled Structures: Monograph", Lira, p. 288, Dnipro, Ukraine, 2017.

[14] A.Ya. Aleksandrov, M.Kh. Akhmetzyanov, "Polarization-Optical Methods Deformable of Solid Mechanics", Nauka, p. 576, Moscow, Russia, 1973.

[15] A.V. Degtyarev, "Missile Technology Problems and Prospects", ART-Press, p. 420, Dnipro, Ukraine, 2014.

[16] V.S. Hudramovich, A.P. Dzyuba, "Contact Interaction and Optimization of Locally Loaded Shell Structures", J. of Mathematical Science - Springer Science, Business Media, Vol. 162, Issue 2, pp. 231-245, 2009.

[17] V.P. Malkov, A.G. Ugodchikov, "Optimization of Elastic Systems", Nauka, p. 288, Moscow, Russia, 1981.

[18] M.I. Reitman, G.S. Shapiro, Methods for Optimal Design of Deformable Bodies", Nauka, p. 268, Moscow, Russia, 1976.

[19] G.V. Reklaitis, A. Ravindran, K.M. Ragsdell, "Engineering Optimization Methods and Applications", John Wiley, Second Edition, New Jersey, USA, 1983.

[20] G.V. Filatov, "Optimal Design of Spported

Cylindrical Shells under Combined Axial Compression and Internal Pressure", J. of Mechanical Engineering, Vol. 24, No. 2. pp, 2021.

[21] A.V. Kondratiev, "The Concept of Optimization of Structural and Technological Parameters of Composite Aggregates of Rocket and Space Technology, Taking into Account the Peculiarities of their Production", Space Science and Technology, Vol. 26, No. 6, Issue 127, pp. 5-22, 2020.

[22] E.V. Binkevich, L.V. Vergeichik, V.I. Mossakovsky, "On the Rational Distribution of the Material of Power Frames of Cylindrical Shells", The VII All-Union. Conferences on the Theory of Shells and Plates, pp. 649-652, Moscow, Russia, 1970.

[23] E.V. Binkevich, A.L. Gashko, V.P. Manza, "To Account for the Strengthening of the Frame of a Cylindrical Shell Loaded with a Radial Force", Appl. Mechanics. Vol. 2. Issue 4, pp. 32-38, 1966.

[24] V.I. Mossakovsky, V.S. Gudramovich, E.M. Makeev, "Contact Problems of the Theory of Shells and Rods", Mashynostroenie, p. 248, Moscow, Russia, 1978.

[25] L.S. Pontryagin, V.G. Bolteanskii, R.V. Gamkrelidze, E.F. Mishchenko, "The Mathematical Theory of Optimal Processes", Interscience, New York. NY, USA, 1962.

[26] A.P. Dzyuba, A. Torskyy, "Algorithm of the Successive Approximation Method for Optimal Control Problems with Phase Restrictions for Mechanics Tasks", J. Mathematical Modeling and Computing, Vol. 9, No. 3, pp. 734-749, 2022.

[27] V.V. Uzhva, "Parameters of Optimal Reinforcement of a Cylindrical Shell in the Area of the Concentrated Influence", The Higher Educational Institutes Mashynostroenie, No. 9, pp. 6-10, 1981.

[28] Ya.M. Grigorenko, G.G. Vlaikov, A.Ya. Grigorenko, "Numerical-Analytical Solution of Shell Mechanics Problems Based on Various Models", Academicperiodical, Kiev, Ukraine, 2006.

[29] V.T. Lizin, V.A. Pyatkin, "Design of Thin-Walled Structures", Mashynostroenie, p. 344, Moscow, Russia, 1985.

[30] A.A. Dzyuba, A.P. Dzyuba, L.D. Levitina, I.A. Safronova, "Mathematical Simulation of Deformation for the Rotation Shells with Variable wall Thickness", Journal of Optimization, Differential Equations and Their Applications, Issue 29, No. 1, pp. 79-95, 2021.

BIOGRAPHIES

Name: **Anatoliy**
Middle Name: **Petrovich**
Surname: **Dzyuba**
Birthday: 30.11.1948
Birth Place: Romny, Ukraine
Master: Mechanics, Mechanical-Mathematical Faculty, Dnipro State University, Dnipro, Ukraine, 1971
Ph.D.: Tech., Structural Mechanics, Dnipro State University, 1977
Doctorate: Dr. Sci., Tech., Deformed Solid Mechanics, 2004
The Last Scientific Position: Prof., Oles Gonchar Dnipro National University, Dnipro, Ukraine, Since 2017
Research Interests: Solid Mechanics, Strength, Stability and Optimal Designs of Construction, Experimental Mechanics, Biomechanics, Inhomogeneous Thin-Walled Structures
Scientific Publications: 195 Papers, 12 Monographs, 30 Patents, 160 Theses

Name:**Ramiz**
Middle Name: **Aziz**
Surname **Iskanderov**
Birthday: 07.07. 1955
Birth Place: Krasnoselo, Armenia
Master: Mechanics, Mechanical-Mathematical Faculty, Baku State University, Azerbaijan, 1977
Ph.D.: Mathematics, Deformed Solid Mechanics, Baku State University, Azerbaijan, 1983
Doctorate: Dr. Sci., Mathematics, Deformed Solid Mechanics, Baku, Azerbaijan, 2014
The Last Scientific Position: Prof., Mechanics Department, Azerbaijan University of Architecture and Civil Engineering, Baku, Azerbaijan, Since]2015
Research Interests: Solid Mechanics; Strength, Stability and Mechanics of Composite Materials, Experimental Mechanics
Scientific Publications: 95 Papers, 2 Monographs, 3 Textbooks

Name: **Yuriy**
Middle Name: **Mikhailovich**
Surname: **Selivanov**
Birthday: 24.07.1948
Birth Place: Panfilov, Kalininsky, Kyrgyzstan
Master: Aircraft Engineering, Mechanical Engineering, S.P. Korolev Kuibyshev Aviation Institute, Kuibyshev, Russia, 1974
Doctorate: Dr. Sci., Tech., Deformed Solid Mechanics, Zaporozhye, Ukraine, 2013
The Last Scientific Position: Prof., Oles Gonchar Dnipro National University, Dnipro, Ukraine, Since 2017
Research Interests: Experimental of Deformed Solid Mechanics, Interference-Optical Methods of Mechanics, Strength, Stability, Oscillations of Inhomogeneous Thin-Walled Structures
Scientific Publications: 127 Papers, 4 Monographs, 5 Patents, 50 Theses